

Immobilization of Ru(II) complex on functionalized SBA-15 and its catalytic performance in aqueous homoallylic alcohol isomerization

Ying Wan^a, Fang Zhang^a, Yunfeng Lu^{b,*}, Hexing Li^{a,**}

^a Department of Chemistry, Shanghai Normal University, Shanghai 200234, China

^b Department of Chemical and Biomolecular Engineering, Tulane University, New Orleans, LA 70118, USA

Received 31 March 2006; received in revised form 8 November 2006; accepted 10 November 2006

Available online 23 November 2006

Abstract

SBA-15-like mesoporous silicas functionalized with high contents of organic amine groups were synthesized by co-condensation of tetraethoxysilane (TEOS) and 3-aminopropyltriethoxysilane (APTES) in the presence of triblock copolymer P123 under acidic conditions. This method provided mesoporous silica with APTES: TEOS molar ratio ranging from 1:15 to 1:6. Further immobilization of dichlorotris(triphenylphosphine)-ruthenium(II) complex onto the functionalized support led to the formation of highly efficient and recoverable heterogeneous catalyst (Ru-AP). Characterizations using XRD, TEM and N₂ adsorption–desorption isotherms demonstrated that the NH₂-modified SBA-15 still retained highly ordered mesopore arrays even after immobilization of ruthenium complexes. Solid state ²⁹Si MAS NMR and ¹³C CP MAS NMR and Raman investigations confirmed the presence of organic amine groups and RuCl₂(PPh₃)₃ complex on silica frameworks. The Ru-AP heterogeneous catalyst exhibited almost the same activity and selectivity as the corresponding RuCl₂(PPh₃)₃ homogeneous catalyst in the water mediated isomerization of 1-phenyl-3-buten-1-ol. The superiority of the Ru-AP was that it could be easily separated from the reaction system and used repetitively without obviously losing activity and selectivity at least for four times.

© 2006 Elsevier B.V. All rights reserved.

Keywords: Green chemistry; Clean isomerization in water medium; Immobilized Ru(II) homogeneous catalysts; NH₂-modified SBA-15

1. Introduction

To maintain a clean world for future generations and sustain a long-term economic growth, considerable efforts have been made to conduct organic reactions in non-polluting media such as water and supercritical CO₂ [1]. Selective transposition of the functionalities of organic compounds is an efficient way in organic synthesis. A typical example is the isomerization of homoallylic alcohols, which has been widely used in synthesizing diverse aromatic compounds for fine chemical, agrochemical, and pharmaceutical applications [2]. At the present stage, most of the aqueous medium reactions involved the use of homogeneous catalysts. Ruthenium complexes, such as RuCl₂(PPh₃)₃, were the most frequently used homogeneous catalysts for 1,3-rearrangement of homoallylic alcohols [3]. Although homogeneous catalysts in general have a higher activity than supported catalysts, they may not be recovered easily,

which may increase costs and lead to heavy-metal pollution in water. It is therefore of great significance to design, synthesize, and apply novel heterogenized homogeneous catalysts, which combine the advantages of homogenous and heterogeneous catalysis.

Organic functionalized mesoporous silicas represented a new class of materials for the design of above-mentioned catalyst, in particular, because their high surface areas, controllable pore structures and tailored pore surface chemistry allowed the binding of a large number of surface chemical moieties [4]. Generally, these mesoporous materials could be synthesized either by a post-modification or by a co-condensation method [4–7]. The latter was proved to be able to prepare functionalized mesoporous silicas with surface ligands that were more amenable and versatile for further immobilization of homogenous catalysts [4].

Surface modification using 3-aminopropyltriethoxysilane (APTES), which could produce terminal amine groups (–NH₂), has been found to be useful for covalent coupling of proteins or organic metals to the silica materials, and showed a potential use in the immobilization of enzymes and organometallic complex [8,9]. Although functionalization of mesoporous sil-

* Corresponding author. Tel.: +1 504 865 5827; fax: +1 504 865 6744.

** Corresponding author. Tel.: +86 21 64322272; fax: +86 21 64874516.

E-mail addresses: ylu@tulane.edu (Y. Lu), hexing-li@shnu.edu.cn (H. Li).

icas with amine groups has been studied by several groups, most of the studies on chelating organometallic complex have been conducted to modify mesoporous silica MCM-41 materials [8,10–12]. Compared with MCM-41, mesoporous silica SBA-15 has much larger pore size, which allowed it to immobilize larger organic metals [13]. It would indeed be vital to achieve amine-functionalized SBA-15 with high contents of organic groups that were highly dispersed within the frameworks and quantitatively accessible for the reactions involving organometallic molecules.

This work reports the synthesis of mesoporous silica SBA-15 functionalized with aminopropyl groups using triblock copolymer P123 (EO₂₀PO₇₀EO₂₀) as a template. We modified the simple co-condensation synthetic method, where tetraethyl orthosilicate (TEOS) and 3-aminopropyltriethoxysilane (APTES) were simultaneously hydrolyzed in the presence of P123, by adding APTES into an acid solution where TEOS was pre-hydrolyzed. A series of functionalized mesoporous silica SBA-15 supports with large pores and tunable contents of aminopropyl groups were achieved. Immobilization of dichlorotris(triphenylphosphine)-ruthenium(II) complex (RuCl₂(PPh₃)₃) generated heterogeneous catalysts. In order to demonstrate their catalytic activities in water, isomerization of 1-phenyl-3-buten-1-ol, an important organic reaction, was examined. The use of water to replace hazardous organic solvent represented a novel direction towards green chemistry.

2. Experimental

2.1. Sample preparation

A typical sample preparation was as follows: a designed amount of TEOS was added to a solution containing 2.0 g P123 and 62.5 ml of 2 M HCl. After stirring at 313 K for 3 h, certain amount of APTES was added into the mixture and the mixture was stirred for 24 h. The molar compositions of precursors were maintained at 1 TEOS:*x* APTES:0.1815 P123:15.05 HCl:152.2 H₂O, where *x* = 0, 1/15, 1/9 and 1/6 for pristine SBA-15, AP15, AP9 and AP6, respectively. The resulting gel was aged at 353 K for 24 h, followed by drying in vacuum at 313 K overnight. The template was removed by extracting with ethanol (500 ml ethanol per gram of as-synthesized material) under reflux for 24 h.

To immobilize Ru(II) complex, 1.0 g of dried AP9 was mixed with a solution of 96 mg of RuCl₂(PPh₃)₃ in absolute toluene. The mixture was stirred overnight at room temperature. It was then washed with toluene, filtered and dried. The dried product (denoted as Ru-AP9) was Soxhlet-extracted with toluene to remove free RuCl₂(PPh₃)₃ and dried in vacuum for another 24 h. Loading of 4.7 wt.% Ru per gram support was established by the analysis of Varian VISTA-MPX inductively coupled plasma optical emission spectrometer (ICP-OES).

2.2. Characterization

The X-ray powder diffraction (XRD) experiments were carried out on a Rigaku D/Max-RB diffractometer with Cu K α radiation. Transmission electron microscopy (TEM) studies

were performed on a JEOL JEM2010 electron microscope, operated at an acceleration voltage of 200 kV. Laser Raman spectra were recorded using a Super LabRam-II spectrometer with a holographic grating of 1800 g/mm, a wavenumber range of 300–3000 cm⁻¹, and a spectral resolution of 2.0 cm⁻¹. The irradiation from a liquid nitrogen cooled He–Ne laser with 632.8 nm wavelength was used for excitation. N₂ adsorption isotherms were measured at 77 K using a Quantachrome Nova 4000 analyzer. The samples were measured after outgassed at 423 K overnight. Pore size distributions were calculated using the BJH model. The specific surface areas (*S*_{BET}) of samples were determined from the linear parts of BET plots (*p/p*₀ = 0.05–0.25). ²⁹Si MAS NMR and ¹³C CP MAS NMR spectra were recorded at 100.6 and 79.5 MHz, respectively, using a Bruker AV-400 spectrometer.

2.3. Activity test

The isomerization of 1-phenyl-3-buten-1-ol in aqueous solution was chosen as a probe to study the catalytic properties of immobilized Ru(II) complex catalysts. The reaction was conducted by stirring 25 mg 1-phenyl-3-buten-1-ol, 5.0 g water, and a certain amount of AP9, Ru-AP9 or RuCl₂(PPh₃)₃ at 373 K for 10 h. The resultants of reaction were extracted with ether and dried by MgSO₄. After filtration and evaporation of solvent, the residue was identified by ¹H NMR spectroscopy. Quantitative analysis was performed on a high-performance liquid chromatograph (Shimadzu SPD-10AVP) equipped with a UV–vis detector and a KR100-5C18 liquid column. The main product was 4-phenyl-3-buten-2-ol, together with a byproduct, 1-phenyl-1-butanone. The reproducibility of all results was checked by repeating the experiments at least three times and was found to be within acceptable limits ($\pm 5\%$).

In order to determine the catalyst durability, the Ru-AP9 catalyst was allowed to settle down after each run of reactions and the clear supernatant liquid was decanted slowly. The residual solid catalyst was re-used with fresh charge of water and reactant for subsequent recycle runs under same reaction conditions. The ruthenium content leached off from the heterogeneous catalyst was determined by ICP analysis.

3. Results and discussion

3.1. Transmission electron microscopy

Fig. 1 showed the TEM images of the amine-functionalized supports AP15 (A and B), AP9 (C and D), AP6 (E and F) and grafted ruthenium heterogeneous catalyst Ru-AP9 (G and H) viewed along [100] (Fig. 1 A, C, E, and F) and [001] (Fig. 2 B, D, F, and H) directions. The well-ordered arrays of mesochannels indicated a typical two-dimensional *p6mm* hexagonal symmetry for all samples [13]. The distances between the centers of mesopores and between the parallel channels were estimated to be about 12.0 and 10.5 nm, respectively. The heterogeneous catalyst with 4.7 wt.% Ru showed a “clean” exterior with retention of the strong image, suggesting that the Ru complex is immobilized uniformly within the mesopores.

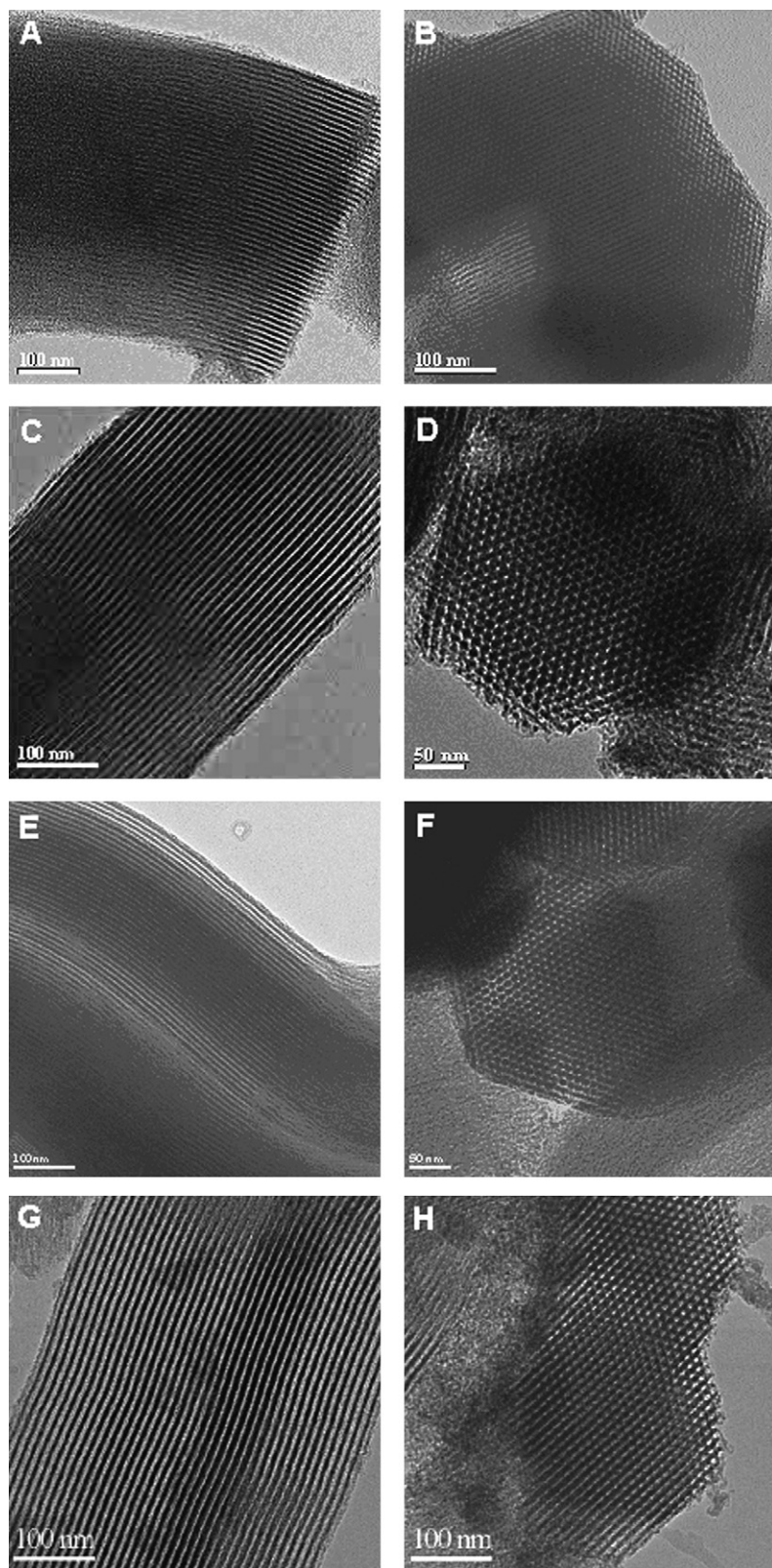


Fig. 1. TEM images of the sample AP15 (A and B), AP9 (C and D), AP6 (E and F) and Ru-AP9 (G and H) viewed along [100] (A, C, E, and F) and [001] (B, D, F, and H) directions.

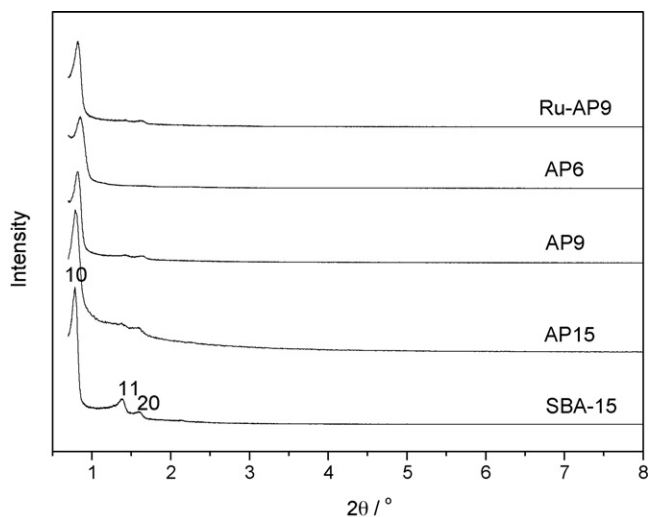


Fig. 2. XRD patterns of pristine and amine-functionalized mesoporous silica samples and immobilized $\text{RuCl}_2(\text{PPh}_3)_3$ catalyst.

3.2. X-ray diffraction

The mesostructures of the functionalized supports and catalyst were further confirmed by the XRD patterns (see Fig. 2). These samples exhibited intense (100) reflections at a d -spacing ranging from 10.0 to 11.0 nm, accompanied by their (110) and (200) reflections, which were consistent with the hexagonal mesostructure observed previously [13]. The unit-cell parameters (a_0) were calculated to be 11.5–12.7 nm, in a good agreement with the values obtained from the TEM images. These well-resolved diffraction peaks indicated a long-range ordered mesostructure to some extent, although broader reflections were observed after the incorporation of a high content of APTES and the anchoring with $\text{RuCl}_2(\text{PPh}_3)_3$.

A featureless XRD pattern in the low angle range of the amine-group functionalized SBA-15 sample, which was prepared by hydrolyzing APTES and TEOS simultaneously in the presence of P123 and aqueous HCl, indicated a disordered mesostructure. Previous works demonstrated that basic amine-containing silanes consistently yielded poorly ordered pore structures compared with neutral materials [10]. The reason may be that the protonation of APTES under the strongly acidic conditions could either cross-link with the surface silanol groups of silicate species or reduce the interactions of the silicate species with P123. This would lead to the disruption of the silicate frameworks, and thus, the formation of a poorly ordered mesostructure. Goldfarb and co-workers [14] also suggested that in the first stage of sol–gel process, hydrophobic inorganic silicates penetrated into the core of polymer packed micelles. Then the hydrolyzed monomers diffused into the corona region forming silicate networks outward. Therefore, the initial hydrolysis stage was very important for the polymerization process of the silicate and the following stages of lengthening and clustering of the micelles, resulting in larger aggregations of the precipitate. Our synthesis was based on the pre-hydrolysis of TEOS in the presence of P123 under acid conditions, resulting in the possibility that relative stable “inorganic network” could

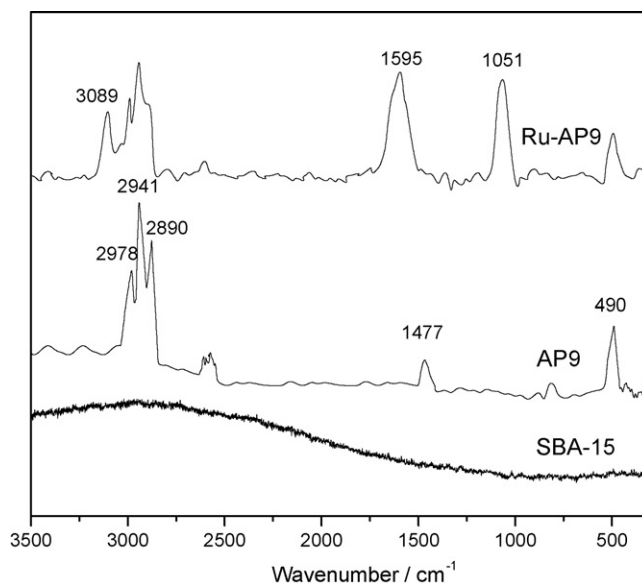


Fig. 3. Raman analysis of pristine, aminopropyl groups functionalized and $\text{RuCl}_2(\text{PPh}_3)_3$ immobilized SBA-15.

be established by co-assembly of P123 and partially hydrolyzed $(\text{EtO})_{4-n}\text{Si}(\text{OH})_n$ species. Such a stable “inorganic network” would be favorable for the incorporation of organic functional groups, even in the case of amine groups with positive charge, and maintenance of the mesostructure. Hence, it was not surprising that the modified method with a delay in adding APTES induced an ordered amine-functionalized SBA-15.

3.3. Raman spectroscopy

The mesoporous silica supports and the Ru(II) catalyst were characterized by Raman spectroscopy, and depicted in Fig. 3. The low intensities scattered by the mesoporous support made it possible to examine the incorporation of aminopropyl groups and the homogeneous $\text{RuCl}_2(\text{PPh}_3)_3$ catalyst, respectively. The comparison of the Raman spectra of AP9 and pristine SBA-15 clearly indicated the incorporation of amine groups. The superpositions of the bands originating from the space molecules were clearly shown at 490, 1477, 2890, 2941 and 2978 cm^{-1} . The former two bands could be assigned to the N–H stretch and the latter three could be attributed to the C–H stretch in aminopropyl groups, respectively [15]. An indication for the ligands exchange, from the comparative studies on AP9 support and Ru-AP9 catalyst, was the bands observed at 1051, 1595 and 3089 cm^{-1} , characteristic for the aromatic C–H stretch, ring stretch and in plane deformation [16]. Thus, it could eliminate any doubt concerning the chemical attachment of homogeneous $\text{RuCl}_2(\text{PPh}_3)_3$ catalyst.

3.4. Solid state NMR

^{29}Si MAS NMR spectra of two selected samples (AP9 and AP6) were shown in Fig. 4. The lines corresponding to the various T^m and Q^n groups could clearly be identified. Q^n represented a silicon atom that connected with n other silicon atoms via oxy-

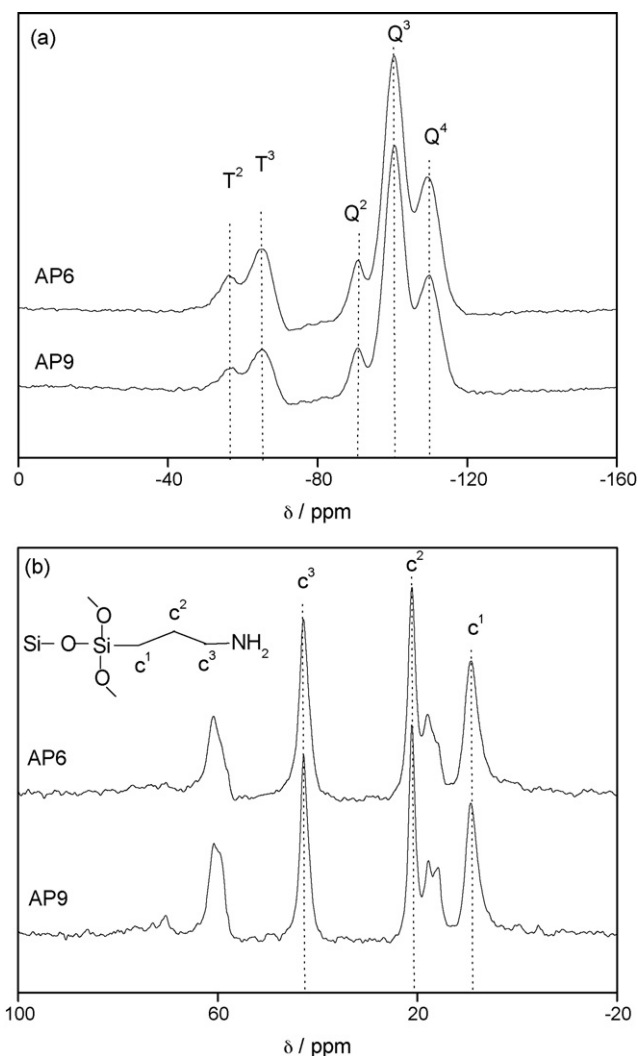


Fig. 4. (a) ^{29}Si MAS NMR and (b) ^{13}C CP MAS NMR spectra of AP9 and AP6.

gen bridges and 4- n silanol groups, whereas T^m showed a silicon atom that bonded with one carbon atom, m other silicon atoms and 3- m silanols. Three resonance signals, Q^4 ($\delta = -110$ ppm), Q^3 ($\delta = -100$ ppm) and Q^2 ($\delta = -91$ ppm), could be observed [17]. The ratios of the signal intensities of Q^4/Q^3 for both samples were similar, indicative of the little destructive effect of high content amine groups on the local structures of silicate frameworks under the experimental conditions [18]. The appearance of T^2 signal at about -56 and T^3 at -66 ppm in both samples was attributed to the cross-linked organosilane APTES, demonstrating the incorporation of the aminopropyl groups within the mesoporous silica frameworks [18,19]. The stronger intensities of the T lines in AP6 than those in AP9 indicated a higher content of amine groups in the former. The $T^m/(T^m + Q^n)$ ratios in the AP9 and AP6 samples were calculated at 0.10 and 0.16, respectively, almost the same as the APTES/(APTES + TEOS) molar ratios in the initial mixture, suggesting that nearly all the APTES incorporated with the TEOS to form NH_2 -modified SBA-15. From ^{13}C CP MAS NMR spectra, one could see that, both the AP9 and the AP6 samples displayed resonance signals at the chemical shifts of 9, 21 and 42 ppm, corresponding to C^1 , C^2

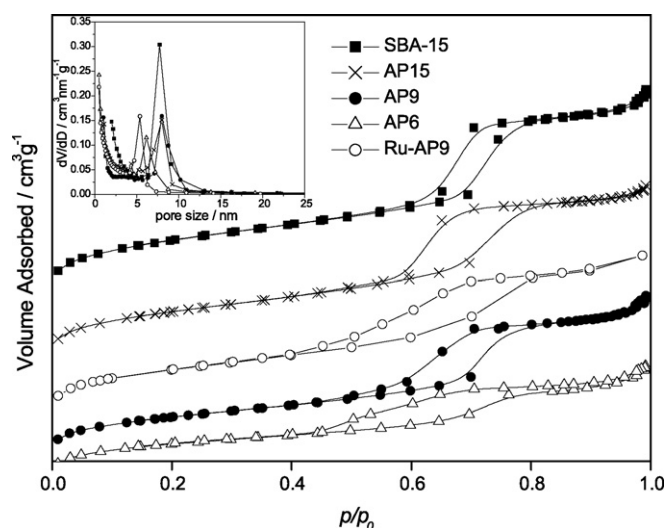


Fig. 5. N_2 adsorption–desorption isotherms and pore size distributions (inside) of amine-functionalized and anchoring Ru complex mesoporous silica samples.

and C^3 atoms in the aminopropyl functional group, further confirming the successful incorporation of organic amino groups on the outer surface and/or the wall of the channels in SBA-15. The peaks around 19 and 60 ppm indicated the presence of the EtOH solvent, which could be easily understood since the samples were washed with EtOH and were not dried in vacuum before NMR characterizations [19].

3.5. N_2 adsorption

Nitrogen adsorption–desorption isotherms (Fig. 5) were measured on all amine-functionalized supports and the Ru(II)-supported catalyst. The detailed pore structure information was listed in Table 1. Like those of SBA-15 mesoporous silica [13], a visible step in the relative pressure at $p/p_0 = 0.7$ or in the vicinity due to the capillary condensation of nitrogen in mesopores, was observed in the isotherms of all samples. With the increase in aminopropyl groups and immobilization of $\text{RuCl}_2(\text{PPh}_3)_3$, less sharp steps were observed than that of pristine SBA-15, indicating broader pore size distributions. Increasing the aminopropyl contents or anchoring with $\text{RuCl}_2(\text{PPh}_3)_3$ led to the reduce the amount of nitrogen uptake due to the decrease in mesopore volumes. However, the decrease in pore volumes and BET surface areas of the functionalized samples were not very distinct in comparison with those of the pure silica SBA-15. The pore walls of all samples were about 5.0 nm in wall thickness, which may provide a good hydrothermal stability [20,21]. The physisorption data indicated further that the regularity of the mesostructures could be maintained to some extent for high contents of aminopropyl groups modification and Ru(II) complex immobilization. It may denote the uniformity in the functional group distributions inside the pore channels, thereby avoiding local clustering of the organic moieties and curtailing necking of the pore channels [16].

Significant variations in N_2 adsorption isotherms were also observed between the two samples of AP6 and Ru-AP9. The latter which has more Ru complex but less amine groups than

Table 1
Physical characteristics of amine-functionalized mesoporous silica materials

Sample	APTES:TEOS (molar ratio)	d_{100} (nm)	S_{BET} ($\text{m}^2 \text{g}^{-1}$)	V_{P} ($\text{cm}^3 \text{g}^{-1}$)	d_{p} (nm)	Wall thickness ^a (nm)
SBA-15	0	11.0	630	0.98	7.7	5.0
AP15	1:15	10.8	580	0.84	8.0	4.5
AP9	1:9	10.5	546	0.77	8.0	4.1
AP6	1:6	10.0	477	0.56	6.2	5.3
Ru-AP9	1:9	10.2	523	0.76	5.4	6.4

^a Calculated by a_0 —pore size ($a_0 = 2d_{100}/\sqrt{3}$).

Table 2
Comparison of catalytic behavior of $\text{RuCl}_2(\text{PPh}_3)_3$ homogeneous catalyst and Ru-AP9 immobilized catalyst for 1-phenyl-3-buten-1-ol isomerization in water medium

Catalyst	Ru-content (mmol)	Conversion (%)	Selectivity (%)	Yield (%)	TON (h^{-1})
$\text{RuCl}_2(\text{PPh}_3)_3$	0.014	79	95	75	0.95
Ru-AP9	0.014	72	91	66	0.87

Reaction conditions—25 mg 1-phenyl-3-buten-1-ol, 5.0 g water, 14 mg $\text{RuCl}_2(\text{PPh}_3)_3$ or 300 mg Ru-AP9 with Ru-loading of 0.47 wt.%, reaction temperature: 373 K, and reaction time: 10 h.

the former showed a sharper capillary condensation step and more uniform mesopore distribution. It was mainly caused by the different contents of aminopropyl groups rather than those of Ru(II) complex. As mentioned above, the destruction of ordered mesostructure by the basic amine-containing silanes was evident. Although the regularity of the mesostructure could be maintained to some extent by the method of pre-hydrolyzed TEOS, the damage by basic APTES should be considered, especially when a large amount of APTES was added. On the other hand, the grafting amount of Ru(II) complex is quite low which shows minor effect on the structural regularity of Ru-AP9 as compared with Ru(II) free sample AP9.

3.6. Isomerization of homoallylic alcohols

Table 2 summarized the catalytic performance of both the $\text{RuCl}_2(\text{PPh}_3)_3$ homogeneous catalyst and the immobilized Ru(II) complex catalyst (Ru-AP9) during the isomerization of 1-phenyl-3-buten-1-ol in aqueous solution. The AP9 itself was inactive for the isomerization reaction, indicating that the Ru(II) complex was the real active center in the isomerization. Besides the unreacted 1-phenyl-3-buten-1-ol, only two products were detected by HPLC analysis. One was the target product, 4-phenyl-3-buten-2-ol; the other is the byproduct, 1-phenyl-1-butanone. As shown in Fig. 6, the selectivity remained almost constant (91%) while the conversion increased almost linearly with reaction time up to 10 h and then remained at 72% when the reaction time further increased. From Table 2, one could see that the heterogeneous Ru-AP9 catalyst exhibited similar conversion, turn-over number (TON) and selectivity as the $\text{RuCl}_2(\text{PPh}_3)_3$ homogeneous catalyst, indicating that the immobilized Ru(II) heterogeneous catalyst behaved similarly as its corresponding homogeneous catalyst. To make sure whether the heterogeneous Ru(II) complex on the PPh_2 -SBA-15 support or the dissolved homogeneous Ru(II) complex was the real catalyst responsible for the present isomerization reaction, the following procedure, proposed by Sheldon et al. [22] was carried out. After

reaction for 6 h in which the conversion exceeded 45%, the reaction mixture was filtered to remove the solid catalyst and then allowed the mother liquor to react for another 20 h under the same reaction conditions. No significant activity was observed, demonstrating that the active species are not the dissolved Ru(II) complexes leached from Ru-AP9. Therefore, it was reasonable to suggest that the present catalysis is heterogeneous in nature. Although the Ru-AP9 heterogeneous catalyst exhibited similar catalytic properties to its corresponding $\text{RuCl}_2(\text{PPh}_3)_3$ homogeneous catalyst, it was more preferable for practical application since it could be easily separated from the reaction system and used repetitively. Table 3 showed the durability of the Ru-AP9 immobilized catalyst during the isomerization of 1-phenyl-3-buten-1-ol in aqueous solution. No significant decrease in the selectivity to 4-phenyl-3-buten-2-ol was observed after being used repetitively for four times. However, the conversion and thus the product yield decreased slightly with the increase in repetitive times. According to ICP analysis, the Ru-content also

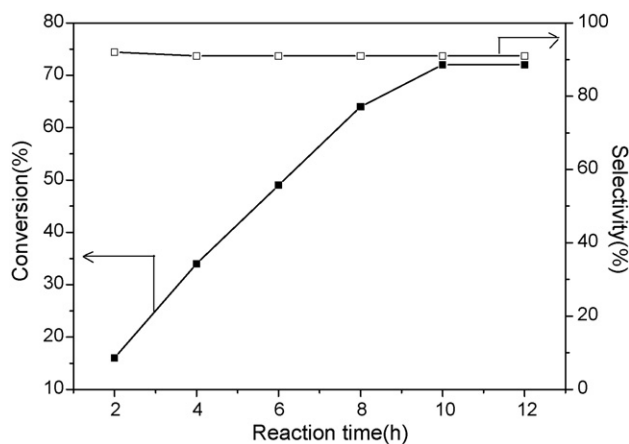


Fig. 6. Dependence of the 1-phenyl-3-buten-1-ol conversion (■) and the selectivity to 4-phenyl-3-buten-2-ol (□) on the reaction time over the Ru-AP9 catalyst. Reaction conditions: 25 mg 1-phenyl-3-buten-1-ol, 5.0 g water, 300 mg Ru-AP9 with Ru-loading of 0.47 wt.%, reaction temperature = 373 K.

Table 3
Change of catalytic behavior of Ru-AP9 immobilized catalyst with its repeated use^a

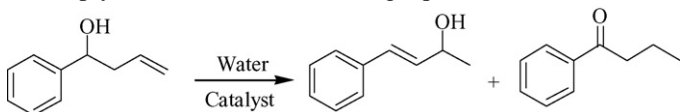
Repeating times	Ru-loading (wt.%)	Ru-content (mmol)	Conversion (%)	Selectivity (%)	Yield (%)	TON (h ⁻¹)
1	0.47	0.0094	59	91	54	0.87
2	0.47	0.0088	56	90	50	0.86
3	0.47	0.0088	54	90	49	0.85
4	0.47	0.0085	52	90	47	0.87
5	0.47	0.0085 + 0.0009 ^b	58	90	52	0.87

^a Reaction conditions: 200 mg Ru-AP9, other reaction conditions are given in Table 1.

^b Supplement of fresh Ru-AP9 containing 0.0009 mmol Ru to make total Ru-content reach 0.0094 mmol.

decreased slightly with the increase in repetitive times while the change of Ru-loading on the AP9 support was not significant. Thus, one could conclude that the decreased Ru-content was mainly attributed to the loss of Ru-AP9 catalyst during its separation from the reaction solution, rather than the leaching of Ru-species from the AP9 support. This was supported by the TON values and also by the fact that the conversion could be recovered when equivalent amount of fresh Ru-AP9 catalyst was supplemented in the system.

According to the product analysis, the reaction route could be simply described in the following equation [3,23,24]:



Regarding the reaction mechanism, it was preferable to apply one which was generalized on a homogeneous catalyst since the anchored $\text{RuCl}_2(\text{PPh}_3)_3$ complex was the active center. Firstly, $\text{RuCl}_2(\text{PPh}_3)_3$ complex coordinated to the olefin. The double bond could be transformed to an internal position, providing an allylic alcohol. Formation of either an allylic alcohol through C–O cleavage or a ketone through C–H cleavage could subsequently occur. The high activity and selectivity of the Ru-PPh₂-SBA-15 catalysts could be attributed to the high surface area of the AP9 support which ensured the monolayer distribution of Ru(II) active sites. Meanwhile, the relatively large size pore in the AP9 may facilitate the diffusion of reactant molecules to contact with the active sites. According to our preliminary studies, the Ru(II) complex immobilized on the NH_2 -functionalized MCM-41 failed in the isomerization perhaps due to its too small pore size (~2 nm). Since the activity and selectivity Ru-AP9 increased with the increase in the NH_2 -content anchored on the support, it was reasonable to conclude that NH_2 -modification of the SBA-15 also played a very important role in promoting catalytic properties. The modification of the SBA-15 surface (including the pore surface) with hydrophobic organic group might favor the adsorption of reactant molecules on the catalyst. Detailed studies are underway.

4. Conclusions

In summary, the present work showed the synthesis of amine-functionalized mesoporous silicas with high-content organic groups. These materials possessed highly ordered mesostructures, uniform pore sizes, high specific surface areas and the

abilities for immobilization of organic metallic complex. During the isomerization of 1-phenyl-3-buten-1-ol to 4-phenyl-3-buten-2-ol in a water medium, which could be considered as a part of green chemistry since no organic solvent was used, and the immobilized $\text{RuCl}_2(\text{PPh}_3)_3$ complex on the as-prepared NH_2 -modified support (Ru-AP9) exhibited high activity and selectivity, almost the same as its corresponding $\text{RuCl}_2(\text{PPh}_3)_3$ homogeneous catalyst. But it could be separated easily from the reaction system and used repetitively for at least four times, showing a good potential in practical application.

Acknowledgments

This work was supported by the National Natural Science Foundation of China (20377031, 20407014 and 20521140450), the Preliminary 973 Project (2005CCA01100), the Shanghai Education Committee (T0402, 04DB05) and the Shanghai Science and technology Committee (06JC14060 and 03QF14037).

References

- [1] C.J. Li, Chem. Rev. 105 (2005) 3095.
- [2] R.A. Sheldon, M.I. Wallau, W.C.E. Arends, U. Schuchardt, Acc. Chem. Res. 31 (1998) 485.
- [3] C. Li, D. Wang, D. Chen, J. Am. Chem. Soc. 117 (1995) 12867.
- [4] M. Kuroki, T. Asefa, W. Whitnal, M. Kruk, C. Yoshina-Ishii, M. Jaroniec, G.A. Ozin, J. Am. Chem. Soc. 124 (2002) 13886.
- [5] X. Liu, B. Tian, C. Yu, F. Gao, S. Xie, B. Tu, R. Che, L. Peng, D. Zhao, Angew. Chem. Int. Ed. 41 (2002) 3876.
- [6] H. Darmstadt, C. Roy, S. Kaliaguine, T.-W. Kim, R. Ryoo, Chem. Mater. 15 (2003) 3300.
- [7] J. Ding, C.J. Hudalla, J.T. Cook, D.P. Walsh, C.E. Boissel, P.C. Iraneta, J.E. O'Gara, Chem. Mater. 16 (2004) 670.
- [8] T. Joseph, S.S. Deshpande, S.B. Halligudi, A. Vinu, S. Ernst, M. Hartmann, J. Mol. Catal. 206 (2003) 13.
- [9] A. Subramanian, S.J. Kennel, P.I. Oden, Enzyme Microb. Technol. 24 (1999) 26.
- [10] A.S. Maria Chong, X.S. Zhao, J. Phys. Chem. B 107 (2003) 12650.
- [11] X. Wang, K.K. Lin, J.C.C. Chan, S. Cheng, Chem. Commun. (2004) 2762.
- [12] K. Mukhopadhyay, A.B. Mandale, R.V. Chaudhari, Chem. Mater. 15 (2003) 1766.
- [13] D. Zhao, J. Feng, Q. Huo, N. Melosh, G.H. Fredrickson, B.F. Chemelka, G.D. Stucky, Science 279 (1998) 548.
- [14] S. Ruthstein, V. Frydman, D. Goldfarb, J. Phys. Chem. B 108 (2004) 9016.
- [15] H. Yang, Y. Yang, Z. Liu, Z. Zhang, Surf. Sci. 551 (2004) 1.
- [16] K. Melis, D. De Vos, P. Jacobs, F. Verpoort, J. Mol. Catal. 169 (2001) 47.
- [17] L. Mercier, T.J. Pinnavaia, Chem. Mater. 12 (2000) 188.
- [18] F. Juan, E. Ruiz-Hitzky, Adv. Mater. 12 (2000) 430.

- [19] H.H.P. Yiu, P.A. Wright, N.P. Bulter, *J. Mol. Catal. B: Enzym.* 15 (2001) 81.
- [20] D. Zhao, Q. Huo, J. Feng, B.F. Chemelka, G.D. Stucky, *J. Am. Chem. Soc.* 120 (1998) 6024.
- [21] Y. Wan, J. Ma, Z. Wang, W. Zhou, *Micropor. Mesopor. Mater.* 76 (2004) 35.
- [22] R.A. Sheldon, M.I. Wallau, W.C.E. Arends, U. Schuchardt, *Acc. Chem. Res.* 31 (1998) 485.
- [23] G.W. Parshall, *Homogeneous Catalysis*, Wiley, New York, 1980, p. 31.
- [24] R.H. Crabtree, *The Organometallic Chemistry of the Transition Metals*, Wiley, New York, 1988, p. 188.